Nonisothermal Crystallization of Isotactic Polypropylene Blended with Poly(α-pinene). 2. Growth Rates

Maria Laura Di Lorenzo,* Sossio Cimmino, and Clara Silvestre

Istituto di Ricerca e Tecnologia delle Materie Plastiche (C.N.R.), Via Toiano 6, 80072 Arco Felice (NA), Italy

Received December 6, 1999; Revised Manuscript Received February 24, 2000

ABSTRACT: The influence of the poly(α-pinene), a natural polyterpene, on growth rate of isotactic polypropylene spherulites was investigated using a dynamic solidification method. It was shown that the use of a constant cooling rate allows the obtainment of reliable growth rate data and permits one to enormously enlarge the range of temperature where crystallization data can be measured. The presence of poly(α-pinene) slows the radial growth rate of polypropylene crystals for all blend compositions investigated (0−50% poly(α-pinene)). Analysis of the experimental data with the Hoffman−Lauritzen model showed that a regime II−III transition is present for plain iPP and for the iPP/PαP miscible blends and that the transition temperature decreases with poly(α-pinene) content.

Introduction

The poly(α-pinene) (PαP), amorphous polyterpene, has been recently proposed as a possible additive to isotactic polypropylene (iPP).[1−5] It was shown that iPP and PαP are partially miscible,[1,2] and their blends have good mechanical properties (blends with PαP content up to 20%) and lower melt viscosity and permeability to gases compared to plain iPP.[3] Studies of isothermal crystallization kinetics of iPP/PαP blends showed that addition of up to 30% of PαP by weight causes a diminution of the radial growth rate of spherulites and of the overall crystallization rate of iPP.[4]

However, solidification during processing of polymers almost invariably occurs under nonisothermal conditions. This raises the question of how solidification rates measured at constant temperatures can be applied to nonisothermal processes,[6] especially when the cooling rate can induce the occurrence of phase separations. This is the case of iPP/PαP blends, whose phase diagram is probably characterized by an upper critical solution temperature (UCST). Hence in these blends, because of a competing effect between onset of crystallization and liquid−liquid phase separation, the cooling conditions determine the phase structure. According to previous investigations,[1,2] when iPP/PαP blends are quenched from the melt, liquid−liquid separation occurs in blends with at least 30% of PαP by weight. When the samples are instead cooled from the melt at 10 °C/min, blends with PαP up to 30% w/w have one homogeneous amorphous phase, whereas the amorphous material of the 50/50 blend results separated in iPP-rich phase and PαP-rich phase.[2] Conversely, isothermal crystallization at 126 °C, which is above the hypothesized UCST, prevents the liquid−liquid phase separation, and the homogeneity of the amorphous phase is retained when the system is cooled to room temperature.[1]

In a previous article on bulk nonisothermal crystallization of iPP/PαP blends,[5] it was shown that the solidification process strongly depends on cooling rate, composition, and miscibility of the components. For the blends with PαP content equal to or lower than 30% w/w, whose amorphous phase remained homogeneous with the cooling rate used, the overall nonisothermal crystallization rate was depressed with respect to plain iPP, because of the diluting effect of the polyterpene. For the 50/50 blend, which presented two amorphous phases, solidification started at temperatures higher than for plain iPP and blends with lower PαP content, since the diluting effect of PαP in the iPP-rich phase was overweighed by an increased number of nuclei that originated from the polyterpene-rich phase domains.

In the present study a nonisothermal crystallization method is used to measure the spherulite growth rates by means of polarized optical microscopy. Chung and Chen suggested an alternative technique to conventional time-consuming isothermal methods:[7,8] according to their investigations, by using one single measurement, it is possible to obtain isothermal solidification data that would require several separate experiments with isothermal methods. In our study the procedure suggested by Chung and Chen is further developed: by using various cooling rates, it is possible to enormously enlarge the temperature range where crystallization data can be obtained. Moreover, using tailored designed nonisothermal temperature programs, the temperature range where growth rate data are measurable can be further expanded.

Experimental Part

Materials. Isotactic polypropylene (iPP) is a commercial product, Shell HY 6100, with $M_w = 3.0 \times 10^5$ g mol^{-1}. Poly(α-pinene) (PαP) is a commercial resin, kindly supplied by Hercules (The Netherlands). PαP derives from the polymerization of α-pinene, which is the main constituent of the wood of coniferous plants. The sample used is Piccolyte A115, with softening point (R&B) = 115 °C, T_g = 61 °C, M_n = 680 g mol^{-1}, M_w = 1075 g mol^{-1}, and M_z = 1650 g mol^{-1} (Hercules data).

The structure of PαP is not exactly known. It is probably constituted by coexistence of two isomers, as shown in the following formula:[9,10]

* To whom correspondence should be addressed. E-mail diloren@irtemp.na.cnr.it.

10.1021/ma992037d CCC: $19.00
Published on Web 04/29/2000

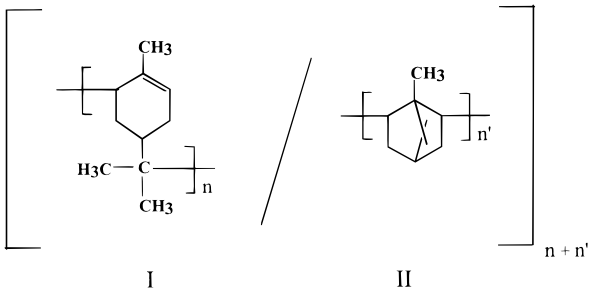

I II

Blend Preparation. Binary blends of polyolefin/resin were obtained by mixing iPP and PαP components in a Brabender-like apparatus (Rheocord EC of HAAKE Inc.) at 210 °C and 32 rpm for 10 min. The mixing ratios of iPP/resin (w/w) were 100/0, 90/10, 80/20, 70/30, and 50/50.

Preliminary experiments performed by thermogravimetric analysis have shown that the blend components do not undergo any thermal degradation in the mixer at the processing conditions used.

Preparation of Compression-Molded Samples. The mixed material was compression-molded in a heated press at a temperature of 210 °C for 5 min, without any applied pressure, to allow complete melting. After this period, a pressure of 100 bar was applied for 5 min. Next, the plates of the press, containing coils for fluids, were rapidly cooled to room temperature by cold water, then the pressure was released, and the mold was removed from the plates.

Optical Microscopy. Crystal growth rates of iPP/PαP blends were investigated by optical microscopy, using a Zeiss polarizing microscope equipped with a hot stage. A compression-molded film, weighting about 0.3 mg, was sandwiched between a microscope slide and a cover glass and then inserted in the hot stage. The thickness of the squeezed sample was less than 10 μm. Each sample was heated from 30 to 200 °C at a rate of 30 °C/min, kept at this temperature for 10 min to allow complete melting, and then cooled to room temperature at various scanning rates, ranging from 0.5 to 8 °C/min. Dry nitrogen gas was purged through the hot stage.

The radius of growing crystals was monitored during crystallization by taking photomicrographs at appropriate intervals of time, using a JVC TK-1085E video camera. Spherulite radii were measured with the software Image-Pro Plus 3.0.

Results and Discussion

The analysis of nonisothermal crystallization from the melt must be performed with care to ensure that the temperature of the sample is properly monitored, as thermal gradients within the sample and between the cooling furnace and the sample can result in a nonexact monitoring of the sample temperature. Moreover, solidification is an exothermic process, and the heat developed during the phase transition may cause some local heating and create additional thermal gradients within the sample. At very high cooling rates the heat evolved by the sample during crystallization can even cause a plateau in the temperature of the sample during a large portion of the solidification process.[11,12] As a consequence of all these thermal lags, transitions can occur at temperatures that do not correspond to those detected by the instrumentation. The thicker the sample, the more critical this problem is.

Few studies relating the influence of sample thickness and cooling rate on the occurrence of thermal gradients during nonisothermal crystallization have been reported in the literature. Monasse and Haudin estimated that, for 300 μm thick polypropylene samples and scanning rates not exceeding 80 °C/min, using a Perkin-Elmer DSC 2B furnace, the thermal gradient between the furnace and the sample is negligible, whereas the thermal gradient within the sample is 1 °C.[13] In a previous article reporting the bulk nonisothermal crystallization of iPP/PαP blends, it was emphasized that, for a same cooling rate, the increase of sample thickness and mass caused shifts of crystallization toward lower temperatures.[5]

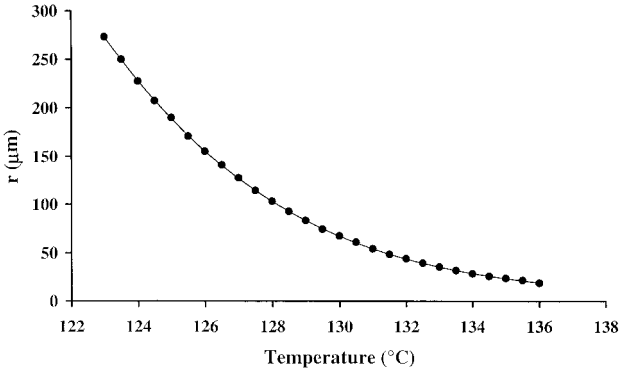

Figure 1. Variation of spherulite radius with temperature for iPP/PαP 90/10 blend during cooling from the melt at 0.5 °C/min.

The samples used in the present study are thinner than 10 μm, and the cooling rates range from 0.5 to 8 °C/min. In such a situation, negligible gradients within the sample and between the furnace and the sample are expected even during solidification, as the heat liberated during crystallization is very low, due to the low sample mass. Hence, it is quite safe to assume that the effective temperature of the sample corresponds to that registered by the hot stage furnace.

Spherulite growth rates, G, are generally measured in isothermal conditions as slopes of the plots of the growing spherulite radius, r, vs crystallization time, t. Chung and Chen suggested a different method to measure G: when solidification is performed at a constant cooling rate, G can be estimated by taking the first derivative of the plot of r vs temperature, T, at each experimental point:[7,8]

$$\frac{dr}{dT} = \frac{dr}{dt}\frac{dt}{dT} \quad (1)$$

where dt/dT is the reciprocal of the cooling rate, and dr/dt is the radial growth rate.

This procedure has been applied to iPP/PαP blends. Spherulite radii have been measured during cooling from the melt at various scanning rates and compositions. Figure 1 reports the variation of r with temperature for the iPP/PαP 90/10 blend cooled at 0.5 °C/min. Similar plots were obtained for other cooling rates and compositions.

In Figure 2 spherulite growth rates of the 90/10 blend obtained using different cooling rates are plotted as a function of temperature. On the same plot G values measured in isothermal conditions, taken from ref 4, are also exhibited. From this plot several features are to be noted:

(1) G data obtained with isothermal and nonisothermal methods are in good agreement.

(2) Each point of the isothermal crystallization curve represents an individual experiment, whereas a single nonisothermal measurement permits one to obtain G values in a wide temperature range.

(3) Data obtained with different cooling rates are well connected to each other.

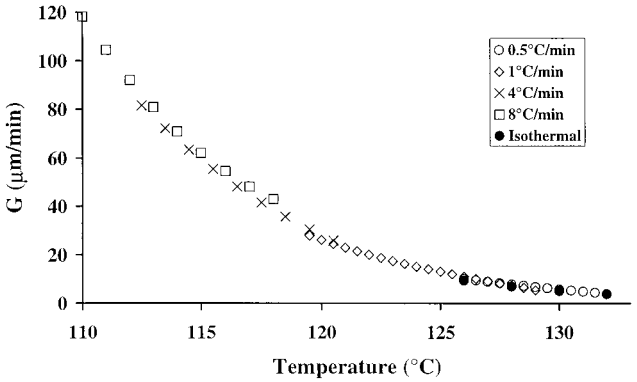

Figure 2. Spherulite growth rate data of iPP/PαP 90/10 blend measured isothermally and at several cooling rates.

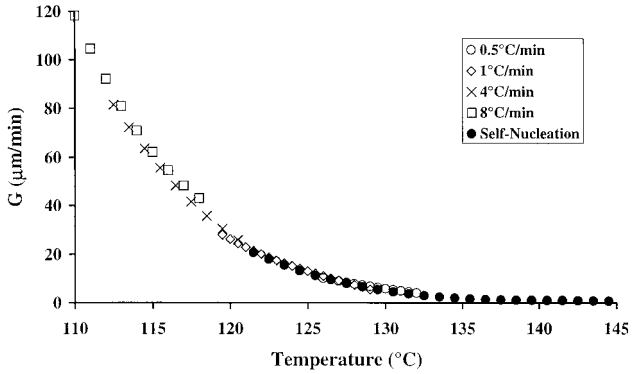

Figure 3. Comparison of *G* data of iPP/PαP 90/10 blend measured during cooling from the melt at 1 °C/min with those measured with the extended procedure after prior nucleation of the crystals.

(4) With nonisothermal crystallization, using different cooling rates, the range of temperatures where *G* is determined is enormously enlarged to lower temperatures with respect to the isothermal method.

The temperature range in which the spherulite radius can be measured has been further enlarged using a self-nucleation procedure, to obtain *G* values at higher temperatures, where nucleation and growth rates are very low. The following temperature program was used. After melting as described in the experimental part, the samples were cooled at 4 °C/min until the first crystalline nucleus was visible by optical microscopy. The temperature was raised again by heating at 10 °C/min up to 160 °C, held for 5 min, and then a cooling at 1 °C/min was performed. During the second cooling the radius of the growing spherulites was recorded as a function of temperature. Growth rate data were calculated as previously described.

The self-nucleation procedure must be used with care, as during formation of nuclei at lower temperatures partial ordering in the melt of some macromolecules could also result. This ordering could persist as a "memory effect" at crystallization temperatures, producing an increase in solidification rate. To verify that the procedure adopted did not alter spherulite growth rate, *G* data obtained with self-nucleation and standard cooling were compared. In Figure 3 this comparison is illustrated for the 90/10 blend. Good agreement between the two sets of data is observed in the temperature range where the data obtained by both methods overlap.

Connecting all *G* data (measured at the various scanning rates and using the self-nucleation procedure), an overall curve of radial growth rate was obtained. In

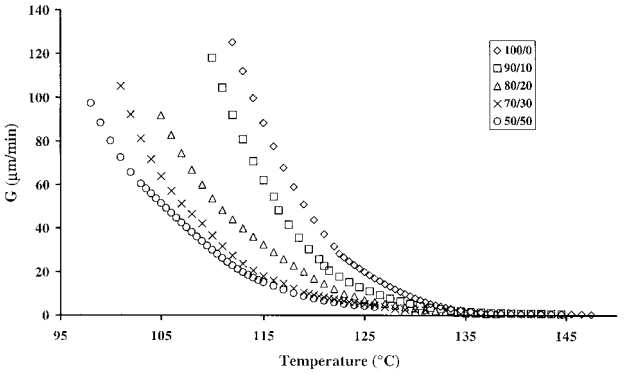

Figure 4. Overall spherulite growth rate data of iPP/PαP as a function of temperature.

Figure 4 the spherulite radial growth rate of plain polypropylene and iPP/PαP blends is reported as a function of temperature. For all samples, *G* decreases with PαP content, in agreement with measurements performed in isothermal conditions.[4]

The decrease of *G* with composition, at a given temperature, can be explained by taking into account the phase structure of the blend. As reported in previous papers, at crystallization temperatures the blends with PαP content up to 30% are miscible,[1,2] whereas the 50/50 blend is phase-separated with the presence of two conjugated amorphous phases.[2]

In the blends that present one homogeneous amorphous phase, PαP affects iPP spherulite growth rate mainly because of diluting effect and melt entropy effect.[14,15] These effects, well described in the literature, produce a decrease in *G*. Spherulite growth rate is influenced also by molecular mobility. In the miscible iPP/PαP blends, the glass transition temperature was reported to increase with the addition of PαP, as the T_g of PαP, 61 °C, is higher than that of iPP.[1,2] On the other hand, at high temperatures, above the melting point of iPP, rheological measurements indicate a strong decrease of the viscosity of the blends with composition, due to the very low molecular weight of PαP. As an example, at 220 °C, for a shear rate of 1 s^{-1}, viscosity drops of about 1 decade going from pure iPP to the 90/10 blend.[3] Unfortunately, at the temperatures where iPP crystallizes, no data on viscosity are available. It can only be hypothesized that in this temperature range the reduction of viscosity upon addition of the oligomer is preserved. The hypothesized higher molecular mobility in the blends facilitates the transport of iPP molecules from the melt to the growing crystals, favoring the growth rate, but is not enough to outweigh the other unfavorable effects.

For the 50/50 blend, which presents amorphous phase separation, an additional energy barrier arises from the effect of domains of the polyterpene-rich phase on the transport term of the macromolecules in the melt. The presence of the domains of PαP-rich phase on the solidification front disturbs spherulite growth. Energy must be dissipated to reject and/or occlude these domains, which constitutes a barrier that opposes solidification, further lowering the growth rate.

Growth rate data of iPP/PαP blends were analyzed with the Hoffman and Lauritzen model.[16]

For a plain polymer, the equation is

$$\ln G + \frac{U^*}{R(T_c - T_\infty)} = \ln G_0 - \frac{K_g}{T_c \Delta T f} \qquad (2)$$

where G_0 is a preexponential term, R is the universal gas constant, U^* is the energy for the transport of the macromolecules in the melt, T_c is the crystallization temperature, T_∞ is the temperature where all the motions associated with the viscous flow stop and is defined as $T_\infty = T_g - C$, where C is a constant that can assume different values, ΔT is the undercooling ($\Delta T = T_m^o - T_c$), and f is a corrective factor that takes into account the variation of the equilibrium melting enthalpy with temperature, defined as $f = 2T_c/(T_c + T_m^o)$. K_g is a term connected with the energy required for the formation of nuclei of critical size, defined as $K_g = nb\sigma\sigma_e T_m^o/\Delta H_m^o k$, where n is a variable that depends on the crystallization regime.[17]

For a binary blend, constituted of a crystallizable and an amorphous component, the expression of the spherulite radial growth rate differs from that of the plain polymer, because of the possible interactions between the two components and of the presence of noncrystallizable material that can modify the motion of the macromolecules in the melt. For these blends the previous equation is so modified:[15,18,19]

$$\ln G - \ln \varphi_2 + \frac{U^*}{R(T_c - T_\infty)} - \frac{0.2T_m^o \ln \varphi_2}{\Delta T} = \ln G_0 - \frac{K_g}{T_c \Delta T f} \quad (3)$$

where φ_2 is volume fraction of the crystallizable component.

Growth of crystals can occur in different regimes, depending on temperature. At high temperatures (low undercooling), formation of a surface secondary nucleus is followed by rapid completion of the substrate; this situation is referred to as regime I. At lower temperatures, in regime II, multiple surface nuclei form on the substrate and spread out slowly. At even lower temperatures, when solidification takes place in regime III, surface nuclei form in such a large number that the distance between two nuclei approximate the width of a stem. Regime III growth is associated with a situation in which the frequency of secondary nucleation exceeds the rate of lateral spreading. Thermodynamically, the rate of lateral growth should be higher than the rate of attachment of a nucleus on the growing surface, because of the lower energy penalty associated with attachment to a niche on the crystal surface. The general understanding is that in regime III, which occurs at temperatures lower than regimes I and II, the mobility of polymer chains is low. The regime II−III transition is diffusion-controlled, in contrast to the regime I−II transition, which is determined by undercooling.[20]

Regime transitions are observed experimentally as abrupt changes of slope in plots of $\ln G + U^*/[R(T_c - T_\infty)]$ (or $\ln G - \ln \varphi_2 + U^*/[R(T_c - T_\infty)] - (0.2T_m^o \ln \varphi_2)/\Delta T$ for the blends) as a function of $1/(T_c \Delta T f)$.[17,20]

Experimental data were analyzed according to eqs 2 and 3, and the results are presented in Figure 5 for two representative compositions. For all samples, the growth rate data fall on two straight lines, supporting distinct regime transition. The slope ratio is very close to 2, as predicted by the theory. The observed break in the plots was taken as an indication of regime II−III transition.

The temperatures at which the regime II−III transition occurs are reported in Table 1. For plain iPP the break in the plot occurs at 138 °C, in good agreement

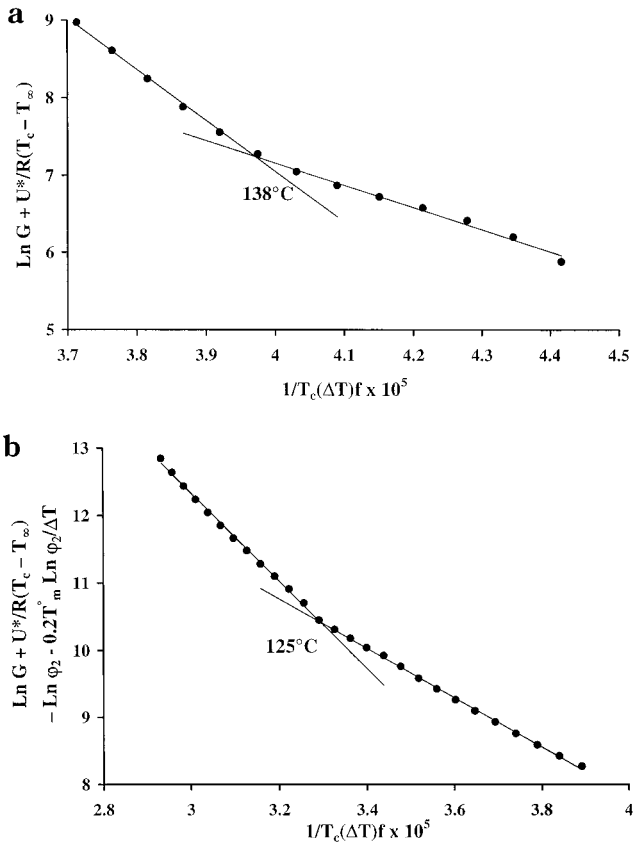

Figure 5. Kinetic analysis of nonisothermal growth data of iPP/PαP blends: (a) 100/0; (b) 80/20. $U^* = 4120$ cal/mol and $T_\infty = T_g - 40$ K were used.

Table 1. Temperature of Regime II−III Transition for iPP/PαP Blends

iPP/PαP (w/w)	T_{II-III} (°C)
100/0	138
90/10	136
80/20	125
70/30	118

with the literature data obtained with conventional isothermal methods.[21−23] For the blends, the regime II−III transition temperature decreases with the addition of PαP, moving from 138 °C for plain iPP to 118 °C for the 70/30 blend.

For iPP/PαP blends the strong reduction of melt viscosity upon addition of PαP is probably preserved at the temperatures where iPP crystallizes. As the temperature of regime II−III transition depends on molecular dynamics, the much higher mobility of iPP chain in the blends, compared to pure iPP, favors the lateral spreading. At the same time, the rate of secondary nucleation decreases with PαP content because of dilution. Both effects cause the shift of the regime II−III transition to lower temperatures with increasing PαP content.

From the slopes of the straight lines, the free energy of folding, σ_e, was calculated, and the values are reported in Table 2. Analysis according to Hoffman and Lauritzen theory was conducted also on isothermally crystallized iPP/PαP blends, as reported in a previous paper.[4] Fairly good agreement is observed between σ_e values measured in isothermal and nonisothermal conditions. For all the samples, the values of σ_e increase with composition. As discussed in ref 4, the increase of σ_e could indicate a decrease of the entropy of folding and

Table 2. Free Energy of Folding Surface, σ_e, for iPP/PαP Blends[a]

iPP/PαP (w/w)	σ_e (erg cm^{-2}) (nonisothermal)	σ_e (erg cm^{-2}) (isothermal)
100/0	178	189
90/10	208	230
80/20	262	291
70/30	291	301

[a] Data measured in isothermal conditions taken from ref 4.

therefore the formation of more homogeneous and regular folding surfaces. As the blends probably have a lower melt viscosity at the crystallization temperatures, the iPP chains can move easily and probably during crystallization can more regularly fold down.

Conclusions

Spherulite growth rate of iPP/PαP blends as a function of temperature can be successfully measured during cooling from the melt. The temperature range where data can be measured, very narrow in the case of isothermal measurements, can be highly expanded using different cooling rates, especially at low temperatures where crystallization is never isothermal. Moreover, using a self-nucleation procedure, it is possible to further enlarge the temperature range toward higher temperatures, where isothermal crystallization is very slow.

This study also shows that the addition of PαP on iPP lowers the radial growth rate of iPP spherulite grown during nonisothermal cooling. For the blends with PαP content up to 30%, which have a homogeneous amorphous phase, this is due to the diluent effect of the polyterpene. For the 50/50 blend, whose amorphous is phase separated, the domains of the PαP-rich phase need to be included and/or occluded in iPP spherulites, which further lowers the iPP growth rate. Moreover, the presence of PαP has a strong influence on the regime II−III transition, which is shifted to lower temperatures with increasing PαP content.

Acknowledgment. The authors thank Mr. G. Loeber of Hercules (The Netherlands) for kindly supplying the poly(α-pinene). This work was partially supported by P.O.P. 1994/1999 Regione Campania, Sottoprogramma 5, Azione 5.4.2, Annualità 1997, Enti Pubblici di Ricerca.

References and Notes

(1) Cimmino, S.; D'Alma, E.; Di Lorenzo, M. L.; Di Pace, E.; Silvestre, C. *J. Polym. Sci., Part B: Polym. Phys.* **1999**, *37*, 867.
(2) Di Lorenzo, M. L.; Cimmino, S.; Silvestre, C.; Wunderlich, B. Manuscript in preparation.
(3) Cimmino, S.; D'Alma, E.; Di Lorenzo, M. L.; Greco, R.; Iavarone, M.; Silvestre, C. Manuscript in preparation.
(4) Silvestre, C.; Cimmino, S.; D'Alma, E.; Di Lorenzo, M. L.; Di Pace, E. *Polymer* **1999**, *40*, 5119.
(5) Di Lorenzo, M. L.; Cimmino, S.; Silvestre, C. *J. Appl. Polym. Sci.*, submitted.
(6) Di Lorenzo, M. L.; Silvestre, C. *Progr. Polym. Sci.* **1999**, *24*, 917.
(7) Chung, C. T.; Chen, M. *Polym. Prepr.* **1992**, *33* (1), 420.
(8) Chen, M.; Chung, C. T. *J. Polym. Sci., Part B: Polym. Phys.* **1998**, *36*, 2393.
(9) Higashimura, T.; Lu, J.; Kamigaito, M.; Sawamoto, M. *Makromol. Chem.* **1993**, *194*, 3441.
(10) Lu, J.; Kamigaito, M.; Sawamoto, M.; Higashimura, T.; Deng, Y. *J. Appl. Polym. Sci.* **1996**, *61*, 1011.
(11) Ding, Z.; Spruiell, J. E. *J. Polym. Sci., Part B: Polym. Phys.* **1996**, *34*, 2783.
(12) Ding, Z.; Spruiell, J. E. *J. Polym. Sci., Part B: Polym. Phys.* **1997**, *35*, 1077.
(13) Monasse, B.; Haudin, J. M. *Colloid Polym. Sci.* **1986**, *264*, 117.
(14) Silvestre, C.; Cimmino, S.; Di Pace, E. In *Polymeric Materials Encyclopedia*; Salamone, J. C., Ed.; CRC Press: Boca Raton, FL, 1996; Vol. 2, p 1595.
(15) Boon, J.; Aczue, J. M. *J. Polym. Sci., Part A-2* **1968**, *6*, 885.
(16) Hoffman, J. D.; Davis, G. T.; Lauritzen, J. I. *Treatise on Solid State Chemistry*; Hannay, N. B., Ed.; Plenum Press: New York, 1976; Vol. 3, p 7.
(17) Hoffman, J. D. *Polymer* **1983**, *24*, 3.
(18) Martuscelli, E. *Polym. Eng. Sci.* **1984**, *24*, 563.
(19) Alfonso, G. C.; Russell, T. P. *Macromolecules* **1986**, *19*, 1143.
(20) Phillips, P. J.; Vatansever, N. *Macromolecules* **1987**, *20*, 2138.
(21) Hoffman, J. D. *Polymer* **1982**, *23*, 656.
(22) Clark, E. J.; Hoffman, J. D. *Macromolecules* **1984**, *17*, 878.
(23) Monasse, B.; Haudin, J. M. *Colloid Polym. Sci.* **1985**, *263*, 822.

MA992037D